Research Square

Preprints are preliminary reports that have not undergone peer review.
They should not be considered conclusive, used to inform clinical practice,
or referenced by the media as validated information.

Etched-Glass Waveguides versus Laminated Filters for Active In-Camera Tint Synthesis

Mateusz Szczęsny
Quantitative Engineering Design (QED)
Jakub Duczmalewski
kontakt@jduczmalewski.com
ATM System sp. z o.o. https://orcid.org/0009-0007-8891-4841
Joanna Starobrat
Warsaw University of Technology
Jarosław Suszek
Warsaw University of Technology
Filip Włodarczyk
Warsaw University of Technology
Maciej Sypek
Warsaw University of Technology

Research Article

Keywords: veiling glare, contrast-reduction filter, planar waveguide, edge-lit illumination, etched glass, tunable tint

Posted Date: September 17th, 2026

DOI: https://doi.org/10.21203/rs.3.rs-11062526/v1

License: This work is licensed under a Creative Commons Attribution 4.0 International License.
Read Full License

Additional Declarations: The authors declare potential competing interests as follows: Jakub Duczmalewski is employed by ATM System, which commissioned the etched-glass filter examined here and commercially rents cinematographic filters and camera equipment. Mateusz Szczesny is employed by Quantitative Engineering Design (QED), the manufacturer of the ScanSpectrum spectrometer used for all measurements reported here. Joanna Starobrat, Maciej Sypek, Jarosław Suszek, and Filip Włodarczyk are with the Faculty of Physics, Warsaw University of Technology. The etched-glass filter was designed and fabricated at CEZAMAT, Warsaw University of Technology. The Tiffen Ultra Contrast filters were

purchased on the open market; the authors have no relationship with The Tiffen Company, which had no role in the design, execution, or reporting of this study. To support independent verification, the underlying spectrometer scans and the analysis code that generates every figure and quantitative value in this paper are available from the corresponding author on reasonable request (see Code, Data, and Materials Availability).

Etched-Glass Waveguides versus Laminated Filters for Active In-Camera Tint Synthesis

Mateusz Szczesny[a], Jakub Duczmalewski[b*], Joanna Starobrat[c], Jarosław Suszek[c], Filip Włodarczyk[c], Maciej Sypek[c]

[a]Quantitative Engineering Design (QED), Górczewska 208/96, 01-460 Warsaw, Poland

[b]ATM System, Wał Miedzeszyński 406, Warsaw, Poland

[c]Faculty of Physics, Warsaw University of Technology, Koszykowa 75, 00-662 Warsaw, Poland

Abstract. Cinematographic contrast-reduction filters spread light from bright image areas into dark ones, lifting shadows and lowering macro-contrast. When mounted in front of a lens and edge-lit by an RGB LED strip, the same filters can act as planar waveguides. In this configuration they add a colored veil to the image, functioning as a tunable tint filter. We report a laboratory comparison of two plate architectures for this role: a custom filter with light-extracting structures etched into glass, and the commercial Tiffen Ultra Contrast family. Five complementary spectrometric measurements were performed: (i) on-axis transmission loss, (ii) veiling glare (haze) against a black background, (iii) spectral shift of edge-injected RGB LED light, (iv) spatial uniformity of the extracted light, and (v) relative extraction efficiency under identical LED drive. The etched-glass filter showed the lowest insertion loss (7.1 % over the 400–700 nm band) and the strongest passive veil, about 1.6 times that of the strongest laminated filter tested. Under identical edge injection its extracted signal was comparable to that same filter, but its RGB balance was near-neutral and stable across the plate, whereas the laminated filters extracted blue-dominant light (center blue-to-red ratio 2.2–3.8) that varied in hue with position. All spectral peak shifts were small ($|\Delta\lambda| \leq 3.5$ nm). We discuss the trade-offs between the two architectures and derive practical guidelines for LED drive-power budgeting and color-shift compensation.

Keywords: veiling glare, contrast-reduction filter, planar waveguide, edge-lit illumination, etched glass, tunable tint

* E-mail: kontakt@jduczmalewski.com

1 Introduction

Veiling glare — a low-spatial-frequency luminous veil cast by stray light — is normally treated as an image-quality defect and measured by standardized methods [1–4]. In cinematography, a controlled veil can instead be useful for lowering macro-contrast and lifting shadow detail [5].

Tiffen describes its Ultra Contrast filters as using ambient light to lighten shadows evenly with little change to highlights [6,7]. In normal use, the strength of the effect is fixed by the chosen grade.

This work concerns an active extension of such glare: the filter plate is edge-lit by a perimeter RGB LED strip, so that the injected light propagates by total internal reflection (TIR) and is extracted toward the camera by scattering from, or diffraction by, structures within the plate. The veil's brightness and color are adjustable during a take, each LED channel using its own slider. The design problem is that of edge-lit light-guide plates, where the distributed extraction features control brightness and uniformity [8,9]. Two architectures are of practical interest:

1. Repurposed commercial contrast-reduction filters (here: Tiffen Ultra Contrast, "UC"), whose *passive* ColorCore laminated construction can also guide edge-injected light [7]. Grades 1/8, 1/4 and 1 were tested (Sec. 2.1).
2. A purpose-built etched-glass waveguide filter (referred to here as the etched-glass (EG) filter), developed at the Centre for Advanced Materials and Technologies (*CEZAMAT*), Warsaw University of Technology, in which the extraction centers are structures etched directly into the glass surface rather than by a proprietary laminated scattering layer.

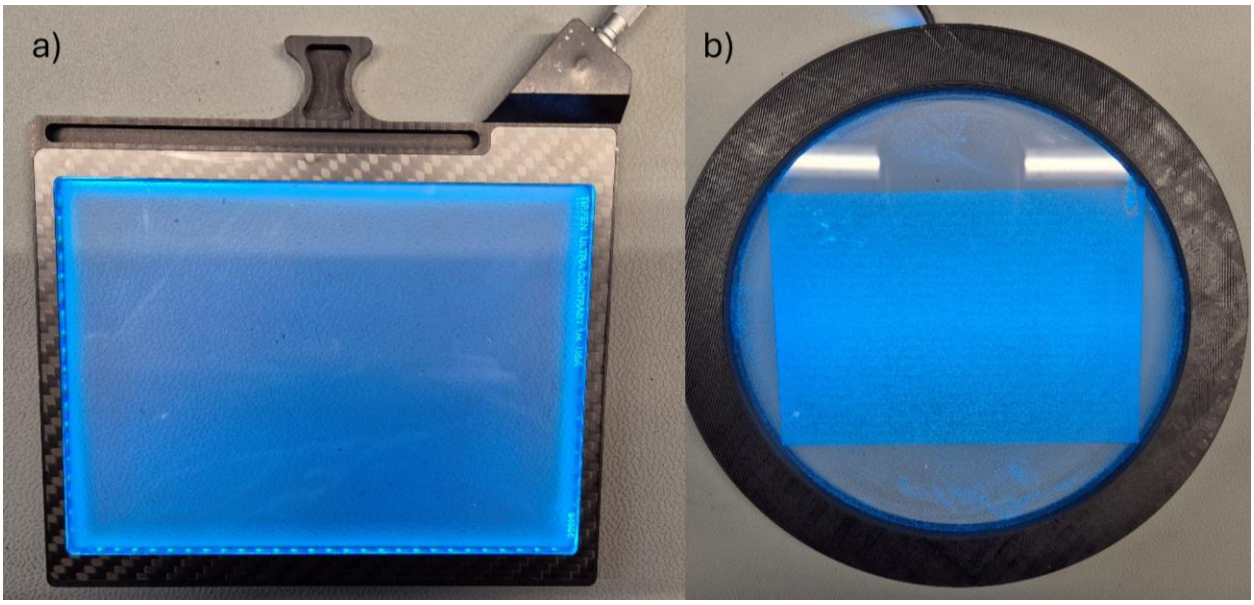


Fig. 1 The two filter architectures under edge illumination, blue channel only. (a) A Tiffen Ultra Contrast filter in the 4 × 5.65-inch cine format, held in a carbon-fiber tray with the RGB LED strip running along the tray aperture. (b) The etched-glass filter in its circular mount, the LED strip following the perimeter of the glass disc; the rectangular etched area is visible as the brighter region at the center.

Figure 1 shows the two filter types mounted and edge-lit. The two architectures are expected to differ in extraction efficiency, spectral neutrality, and spatial uniformity. The UC filters are engineered for passive imaging rather than as light-guide plates, so their scattering is weak and broadly neutral. When edge-lit, much of the injected flux is expected to leave outside the acceptance cone of the lens or continue to the opposite edge. A purpose-designed etched pattern can in principle send more light toward the lens and spread extraction across the aperture. On the other hand the etched structures may also introduce diffraction artifacts that a random scattering medium is less likely to produce.

Edge-lit light-guide plates widely used in display backlighting [8–10] and illuminated in-camera filter assemblies have been patented [11], but to the best of our knowledge neither architecture has been characterized quantitatively in this role, and no published comparison exists between a purpose-built waveguide filter and a repurposed contrast-reduction filter. This paper provides such a comparison, including a five-part measurement protocol, quantitative results for one EG filter and three UC grades (1, 1/4, 1/8), a mapping of the EG filter onto the UC grade scale, and practical guidelines for LED power budgeting and per-channel color-shift compensation.

2 Filter Architectures

2.1 Tiffen Ultra Contrast Filters

Tiffen describes the UC filters as ColorCore laminated filters that use ambient light to reduce contrast by lightening shadow areas while leaving highlights largely unchanged [6,7]. The important characteristic for the present experiment is that the UC stack contains a weak, randomly distributed scattering pattern that can also extract edge-injected light. In the 4 × 5.65-inch cine format used here the filters are sold in grades 1/8, 1/4, 1/2 and 1. The contrast reduction effect roughly doubles with each step. Grades 1/8, 1/4 and 1 were tested. Tiffen does not publish the composition or size distribution of the contrast-reducing medium, so we treat it as a proprietary scattering layer rather than assigning a particle model.

In the edge-lit configuration used here, the laminated stack can act as a planar waveguide. LED light injected at the edge is partially trapped by TIR, and the filter's distributed scattering mechanism extracts part of this guided light toward the camera lens.

2.2 Etched-Glass Waveguide Filter

In contrast to the proprietary laminated medium of the UC family, the EG extraction centers are waveguide structures etched into the glass itself, following e.g. the mask-and-etch approach established for all-glass light-guide plates [10], and are designed to guide light from the LED-lit perimeter toward the interior and spread the extracted veil more evenly across the aperture. A purpose-designed extraction pattern can therefore improve both uniformity and efficiency, but periodic or quasi-periodic structures may also create diffraction artifacts.

The EG filter was designed as a random-phase structure with variable fill-factor (Fig. 2). The filter consists of an array of square micro-patches, each with a stochastic position within a nominal lattice cell of approximately 71.7 μm pitch. Each patch is filled with 1 μm pixels of random local etch depth, forming a random-phase structure. The patch side length of patches varies smoothly along one axis only—from about 20 μm at the edges to 51 μm at the center, yielding a fill-factor that rises from roughly 8 % to 51 %. This one-dimensional gradient compensates for the decay of edge-injected light across the aperture. The patch density is constant across the device (about 200 patches per mm^2), so fill-factor is determined solely by patch size. The random placement mitigates periodic artifacts such as diffraction and moiré patterns. Fabricated by electron-beam lithography on a 200 mm wafer, the active area forms a rectangle of roughly 133 × 104 mm, with feature sizes down to ~1 μm. Profilometry of the fabricated plate (Fig. 3) confirms the design. Segmenting the seven surface maps of the December 2022 CEZAMAT survey gives 543–556 patches per 2.1 × 1.3 mm field, constant to ±1.2 %, so coverage is carried by patch size alone at a fixed lattice density. The measured square sides rise from 26.1 μm near the edges to 45.1 μm at the plate center, within the designed 20.5–51.2 μm range demanded of the mask. The height traces give a surface relief of 0.52–0.79 μm inside the patches against a field flat to 54 nm peak-to-valley.

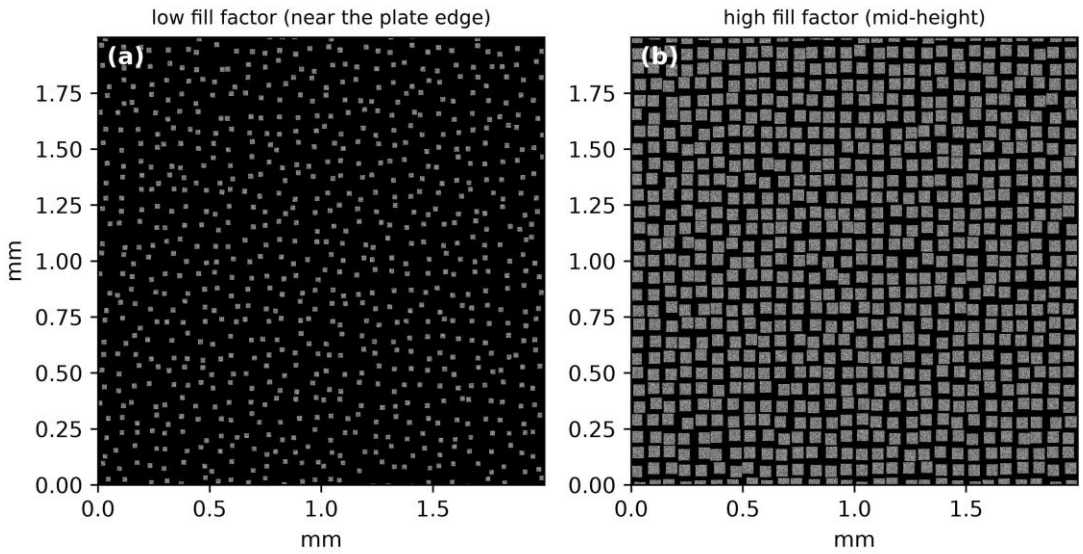


Fig. 2 Selected areas of the design of the EG filter, extracted from selected areas of the design: (a) a low-fill-factor area near the top edge of the plate and (b) a high-fill-factor area at mid-height. The extraction centers are square micro-patches filled with a 1 µm-grain random-phase texture, one per 71.7 µm cell and placed stochastically within it. Between (a) and (b) the patch side grows from 20.5 µm to 51.2 µm while the number of patches per unit area stays constant.

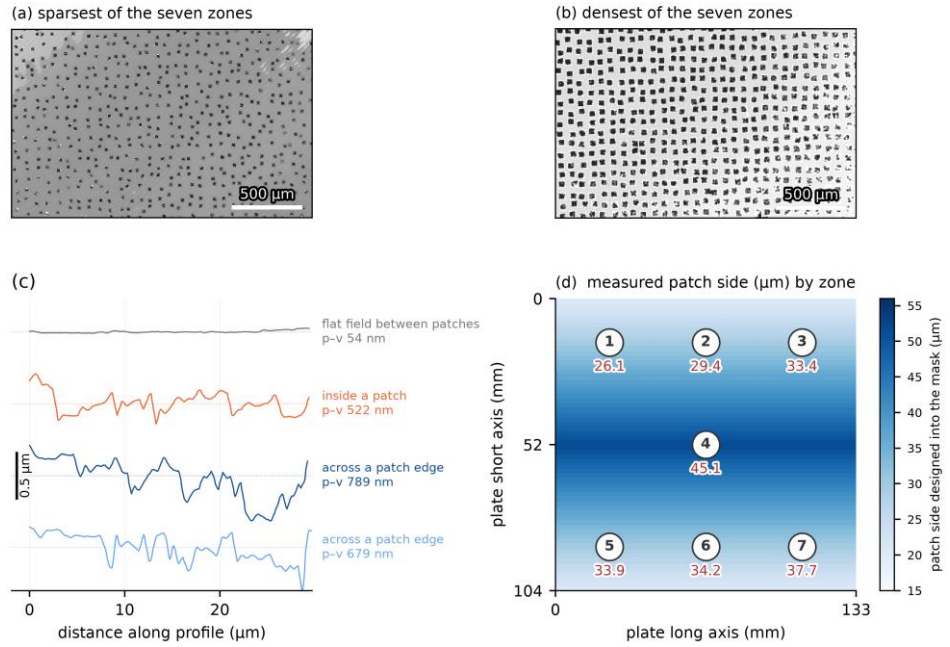


Fig. 3 Profilometry of the fabricated EG plate. (a), (b) Surface maps at the sparsest and the densest of the seven surveyed zones respectively, over equal 2.1 × 1.3 mm fields, shaded by relative height within each map's own instrument range. (c) Height profiles digitized from the report and offset vertically; the bar gives the common height scale. (d) Square side measured in each zone (µm, in red).

3 Experimental Methods and Results

All measurements were performed with a ScanSpectrum portable VIS–NIR spectrometer with 3 nm full width at half maximum (FWHM) spectral resolution in light source measurement mode [12]. This mode measures the emission spectrum of an external light source and covers the 350–1100 nm spectral range. The spectra were recorded at 0.25 nm intervals in a darkened laboratory. For the edge-lit tests, a strip of individually dimmable RGB LEDs was attached around the perimeter of the tested filters, with the brightness of each channel adjustable independently. Five filter conditions were compared throughout: (1) no filter (baseline), (2) EG filter, (3) UC 1, (4) UC 1/4, and (5) UC 1/8. Each condition was measured in n = 3 repetitions unless stated otherwise. Scalar comparisons are reported as averages over the visible range (400–700 nm): each quantity is formed from the band-integrated signal rather than read at a single wavelength. The integration weights every wavelength by the flux the source delivers there, so the band edges, where the source is dim, contribute little and the result does not depend on an arbitrarily chosen reference wavelength. Uncertainties and error bars in the graphs presented for each measured condition denote ±1 standard deviation (sd) over repetitions.

3.1 Test 1: On-Axis Transmission Loss

Method. A stabilized light source was aimed so that the light passes through the tested filters and into the spectrometer measurement channel. This quantifies the passive insertion loss the filter imposes on scene light, both spectrally and as a band average.

Results. Table 1 and Figure 4 summarize the transmission results. All filters removed less than 10 % of the on-axis light across the visible band. The EG filter showed the lowest loss (92.9±0.3 % relative transmission), with UC transmission decreasing weakly with increasing grade (91.13±0.08 % for 1/8 down to 90.2±0.5 % for grade 1).

Figure 4 reveals a qualitative difference: the EG transmission is flat (≈93 %) across the visible band, whereas the UC transmission peaks near 500 nm and declines steadily toward longer wavelengths, losing a further 3 to 4 percentage points by 700 nm. This preferential attenuation of longer wavelengths is consistent with the blue-shifted peaks observed in Test 3 (Sec. 3.3).

Table 1 Relative transmitted intensity integrated over the 400–700 nm band (mean ± sd, n = 3). The unfiltered baseline defines 100 % and so carries no ± of its own; its repeatability over repetitions, ±0.5 % of the band-integrated signal, matches the spectral scatter shown as a gray band in Fig. 4 and sets the scale on which the filter values should be read.

Filter	Relative transmission (%)	Insertion loss (%)
No filter	100.0	—
EG	92.9 ± 0.3	7.1
UC 1/8	91.13 ± 0.08	8.9
UC 1/4	90.6 ± 0.3	9.4
UC 1	90.2 ± 0.5	9.8

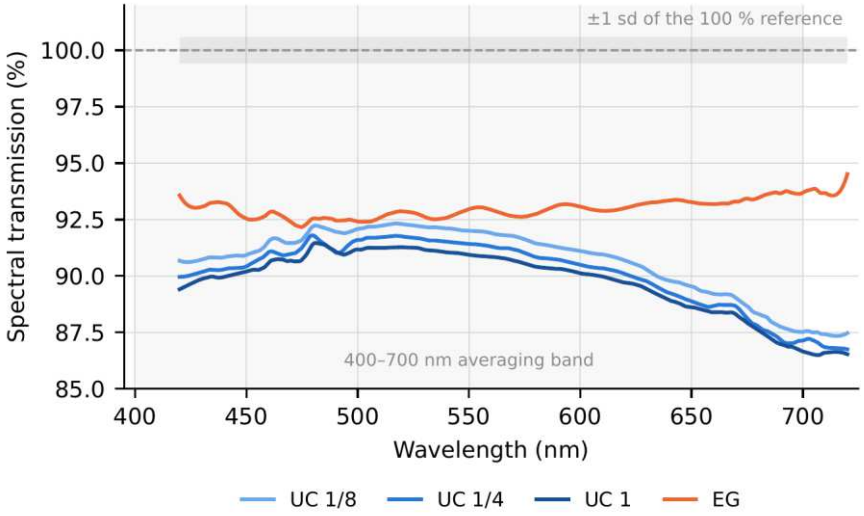


Fig. 4 On-axis transmission relative to the unfiltered baseline (Savitzky–Golay smoothed; the shaded span marks the 400–700 nm averaging band; the gray band is the ±1 sd repeatability of the unfiltered scans that define 100 %); n = 3.

3.2 Test 2: Veiling Glare (Haze) on a Black Background

Method. The filter was mounted against a black background with the light source positioned off-axis on the same side of the tested filter as the spectrometer such that only light scattered by the filter reaches the spectrometer. The haze signal H is expressed as a percentage of the direct source signal S_{direct}, all three signals integrated over the 400–700 nm band, after subtracting the no-filter background ($S_{nofilter}$) of the black-background geometry from the measured signal (S_{filter}):

$$H = 100\% \times \frac{\int_{400}^{700} \left(S_{filter}(\lambda) - S_{nofilter}(\lambda)\right) d\lambda}{\int_{400}^{700} S_{direct}(\lambda) d\lambda}. \quad (1)$$

The EG filter was measured with n = 6 repetitions in this test.

Results. Figure 5a shows the haze signal, Eq. (1), integrated over the visible band. The EG filter produced the strongest veil (0.566±0.092 % of the direct source signal), followed by UC 1 (0.343±0.012 %), UC 1/4 (0.078±0.007 %), and UC 1/8 (0.038±0.005 %); the no-filter control is zero by definition, with a repeatability of ±0.004 %.

Within the UC family, haze increases linearly with the manufacturer-declared grade (Fig. 5b): a least-squares fit gives $H = 0.350\ s - 0.007$ (as a percentage of the direct source), where s is the declared grade, with $R^2 = 0.9999$. With three points and two free parameters the fit has a single degree of freedom, so this R^2 shows that the three grades are mutually consistent rather than establishing linearity over the whole grade scale. Inverting the fit for the EG filter yields an equivalent UC grade of 1.64±0.27 — an extrapolation beyond the highest grade measured — i.e., the EG veil is about 1.6× that of the strongest UC grade tested. Propagating the measured haze uncertainties together with the fit-parameter covariance by Monte Carlo bounds the equivalent grade at 1.1–2.2 (95 % confidence), so the extrapolation is wide but not unbounded. The EG filter also exhibited the largest measurement spread (relative sd ≈16 % versus ≈3.4 % for UC 1), consistent with its lower spatial uniformity (Sec. 3.4).

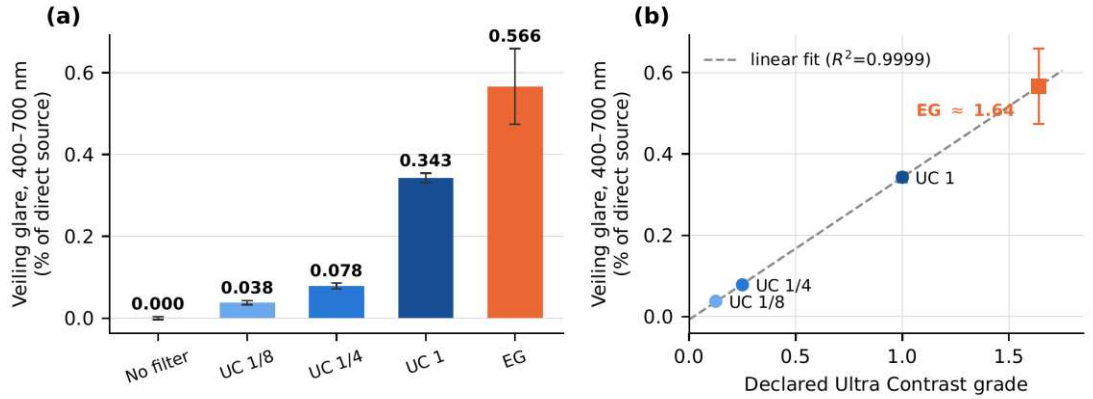


Fig. 5 Veiling glare (haze) on a black background. (a) Haze integrated over the 400–700 nm band, as a percentage of the direct source signal, Eq. (1); error bars: ±1 sd (n = 3; n = 6 for EG). (b) Haze versus declared Ultra Contrast grade with linear fit ($R^2 = 0.9999$); placing the EG filter on the fitted line yields an equivalent grade of ≈1.6, extrapolated beyond the fitted range.

3.3 Test 3: Spectral (Color) Shift of Edge-Injected LED Light

Method. The red, green, and blue channels of the edge-mounted LED strip were each measured twice: directly (baseline spectra; peak wavelengths 635.9±1.4, 521.2±0.3, and 466.1±0.2 nm for R, G, B; n = 2–4 after the rejection described below) and at the plate center after propagation through and extraction from the filter (n = 3–4 per filter and channel). The same LED strip was used for all filters and for the baselines, so shifts are directly comparable across filters. Peak positions were determined per repetition from Savitzky–Golay-smoothed spectra (10 nm window, 3rd order) with parabolic sub-sample interpolation, and the shift is the difference of mean test and mean baseline peak positions. The absolute intensity of the direct-LED scans varied strongly between repetitions, because the usable exposure window is narrow; repetitions that reached the sensor ceiling (signal >1.9) or stayed below 0.05 were rejected. The two red baselines that passed this screening still differ by 1.9 nm, and this spread dominates the ≈±1 nm uncertainty of the red-channel shifts. LED warm-up and multi-channel drive both shift the bands toward longer wavelengths by a few nanometers, so all shifts reported here compare single-channel filter scans against single-channel baselines of the same strip; the uniformity scans were used only for intensity, not for peak position.

Results. Peak-position shifts of the extracted LED light relative to the shared direct-LED baselines are shown in Fig. 6 and Table 2. All shifts are small, $|\Delta\lambda| \leq 3.5$ nm, i.e., of little visual consequence for a tint filter, but the channel-by-channel pattern differs between the two families:

For UC 1 and UC 1/4, a blue shift is present in every channel, growing toward the red, as expected from the declining long-wavelength transmission of the laminated stack (Fig. 4).

In both the EG filter and UC 1/8 shifts do not exceed 2 nm, but are not uniformly consistent with zero. All three EG channels are red-shifted, so the filter is better described as slightly red-shifted than as shift-free, and its green value, taken in the pre-fix session, is not directly comparable. UC 1/8 is mixed: red and blue red-shifted, green blue-shifted like the denser grades — a pattern we cannot explain and report as unresolved.

This measurement is highly sensitive to the LED reference: an earlier series that used separate LED sets for the EG and UC filters suggested UC shifts several times larger, which the shared-baseline measurement reported here does not reproduce.

Table 2 Shift of the spectral peak position of extracted LED light at the plate center relative to the shared direct-LED baseline (negative = toward shorter wavelengths; mean ± combined standard error). The EG green channel was measured in the pre-fix session. The coupling change itself does not shift a peak, but the drive and thermal state of that session differ (see the Method above), so the EG green value is not directly comparable with the other two EG channels. The ±0.2 nm uncertainty quoted for that channel is the within-session repeatability and does not include the session-to-session systematic, which the Method above shows to be of the same order as the shift itself.

Filter	Red LED (nm)	Green LED (nm)	Blue LED (nm)
EG	$+1.8 \pm 1.0$	$+1.4 \pm 0.2$	$+0.7 \pm 0.1$
UC 1	-2.9 ± 1.0	-2.2 ± 0.2	-0.6 ± 0.1
UC 1/4	-3.5 ± 1.0	-2.6 ± 0.3	-1.1 ± 0.1
UC 1/8	$+1.1 \pm 1.0$	-2.0 ± 0.6	$+0.5 \pm 0.1$

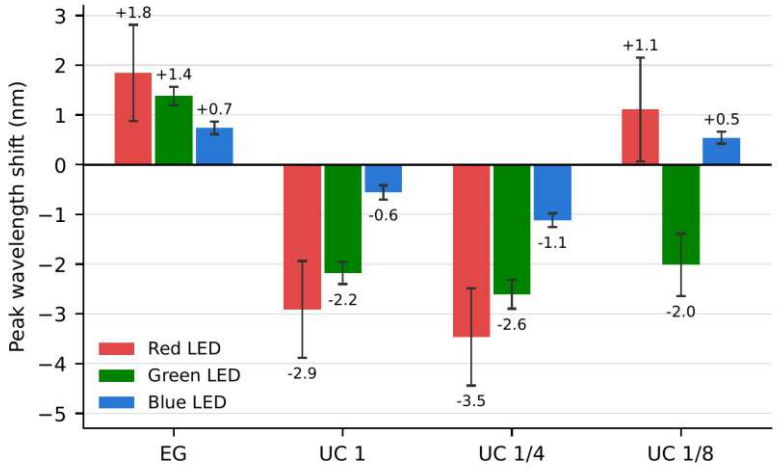


Fig. 6 Shift in spectral peak position relative to the shared direct-LED baseline for red, green, and blue LED channels. Error bars: combined standard error of the test and baseline peak positions. All shifts are within 3.5 nm; UC 1 and UC 1/4 are blue-shifted with the magnitude growing toward the red.

3.4 Test 4: Spatial Uniformity of Extraction

Method. The extracted light was sampled on a 3 × 3 grid covering the filter surface (corners, edge midpoints, and center), with all three LED channels lit and the same strip and drive settings for every filter; n = 2–4 scans per grid position. For each scan the R, G, and B peak heights were read in the 600–690, 495–560, and 430–490 nm bands. Their sum serves as the total-extraction metric,

and the per-channel values yield channel-resolved uniformity maps. Mean values for each position were normalized per filter to the brightest position.

Results. Figure 7 shows the nine-point uniformity maps (total-extraction metric, normalized per filter to the brightest position). The two architectures have opposite spatial signatures.

For the EG filter, extraction peaks at the plate center (1.00) and falls to 0.43–0.58 at the corners (min/max = 0.43), but the field is not radially symmetric: it is a band running along the long axis of the plate. Averaged by row, the mid-height points are 1.62× brighter than the top and bottom rows (0.87 against 0.54 and 0.53), whereas averaged by column the center exceeds the left and right thirds by only 1.11× (0.69 against 0.64 and 0.61). This is the signature of the one-dimensional coverage grading of Sec. 2.2, whose axis coincides with the measured band. The grading therefore does carry light into the interior, and slightly overcompensates the natural edge-brightness of an edge-lit plate along the axis it acts on, while the orthogonal axis is left uncompensated by this design. The three UC filters show no comparable anisotropy (both ratios within 0.83–1.03).

For the UC family, extraction peaks at a corner or the top edge and is weakest toward the center-right and bottom-right. The lower grades are flatter than UC 1, with UC 1/4 flattest overall (UC 1/4: min/max = 0.76; UC 1/8: 0.68; UC 1: 0.54). This is consistent with weaker scattering allowing guided light to spread deeper into the plate before extraction. The flattening is not strictly monotonic in grade: UC 1/8 is less flat than UC 1/4 in every channel, which we attribute to plate-to-plate variation rather than to scattering strength.

The channel-resolved data refines this picture. For the UC filters the red channel is extracted far less uniformly than blue (min/max 0.29 versus 0.63 for UC 1; 0.44 versus 0.72 for UC 1/8), while green tracks blue closely (0.65 and 0.71), so red is an outlier rather than one end of a smooth spectral trend — as expected since the long-wavelength absorption (Fig. 4) attenuates guided red light fastest. The UC veil is therefore redder near the strong-extraction edge and bluer elsewhere. The EG filter shows no such divergence (0.42–0.45 in all three channels), so its veil color is position-independent even though its brightness is not.

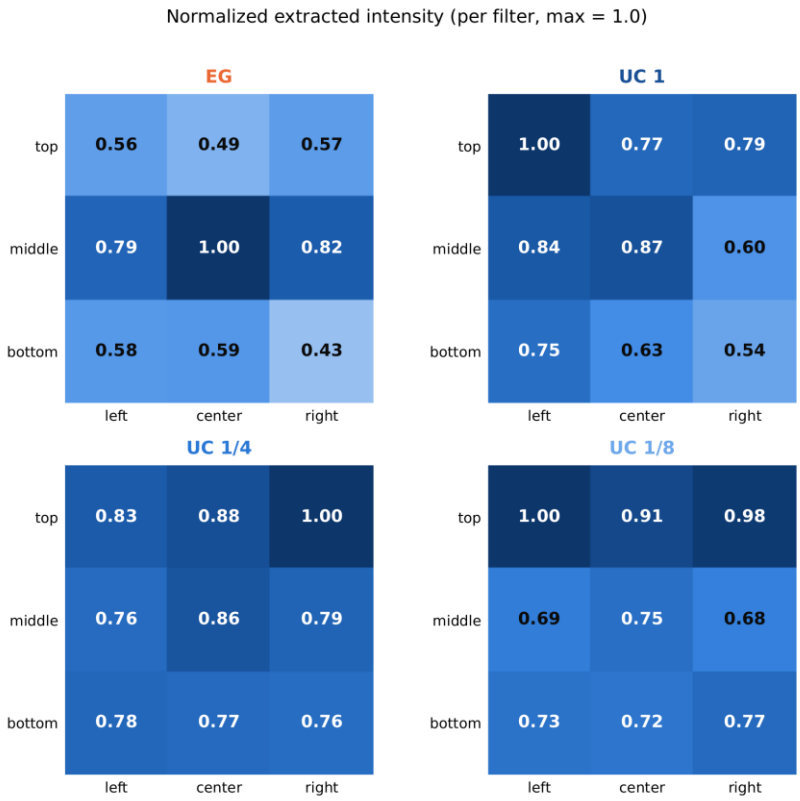


Fig. 7 Nine-point uniformity maps of the intensity of the total extracted signal (per-filter normalization, brightest position = 1.0; mean of n = 2–4 scans per cell, all three LED channels lit, identical strip and drive for all filters). The EG filter shows a bright band along its long axis, set by the one-dimensional grading of its extraction pattern; the UC family is edge/corner-weighted, flattening as the grade decreases toward 1/4.

3.5 Test 5: Relative Extracted Luminosity on a Black Background

Method. Because the uniformity test (Test 4) used the same LED strip and drive settings for every filter, its absolute signal levels also provide a direct cross-filter comparison of extraction toward the camera: per-channel peak heights at the plate center, and the total-extraction metric averaged over all nine positions. This compares the filters against each other under identical injection; it is not an absolute extraction efficiency, since the flux actually coupled into each plate edge was not measured. The EG series was repeated after a fault in the LED strip was corrected (in the first session only the red channel was lit); the post-fix values are used here, and the coupling caveat this raises is explained below.

Results. Because all filters were measured under identical LED drive, the absolute extracted signals compare the architectures directly (Fig. 8). Averaged over the nine positions, the total extracted signals of the EG filter and UC 1 are comparable (ratio ≈1.1) — a difference far smaller

than the coupling uncertainty described below. Within the UC family, where the same strip was used throughout, the ratios relative to UC 1 are 0.59 (UC 1/4) and 0.51 (UC 1/8). Two observations follow:

Grade scaling is compressed. Passive haze spans a factor of about nine across the UC family (Sec. 3.2), but edge-lit extraction spans barely a factor of 2. Strong scattering extracts guided light close to the injection edge at the expense of the interior, so the position-averaged output saturates with grade.

Channel balance differs strongly. At the plate center UC extraction is blue-dominant — blue-to-red 2.2 (UC 1), 3.6 (UC 1/4), 3.8 (UC 1/8) — against 1.1 for the EG filter, with the green-to-red ratios intermediate (0.99, 1.58, 1.64 versus 0.66). The largest uncertainty on any of these ratios is ±0.12 (±1 standard error of the mean (sem), n = 3). Relative to the EG reference, UC 1 extraction is enriched 1.5× in green and 2.0× in blue: a monotonic ordering in wavelength, as expected if the dominant effect is wavelength-dependent loss along the guided path. Both ratios rise as the UC grade falls, because weaker scattering lets the light travel farther before extraction. Matching a target tint through a UC plate therefore needs a substantial red boost that, since the red deficit grows away from the injection edge, is exact at only one position.

The EG caveat described above applies: single-color scans taken before the LED-strip fix were ≈2.2× brighter than after it, so the EG-to-UC ratio is uncertain by the change in strip-to-edge coupling; the quoted ratio uses the post-fix session.

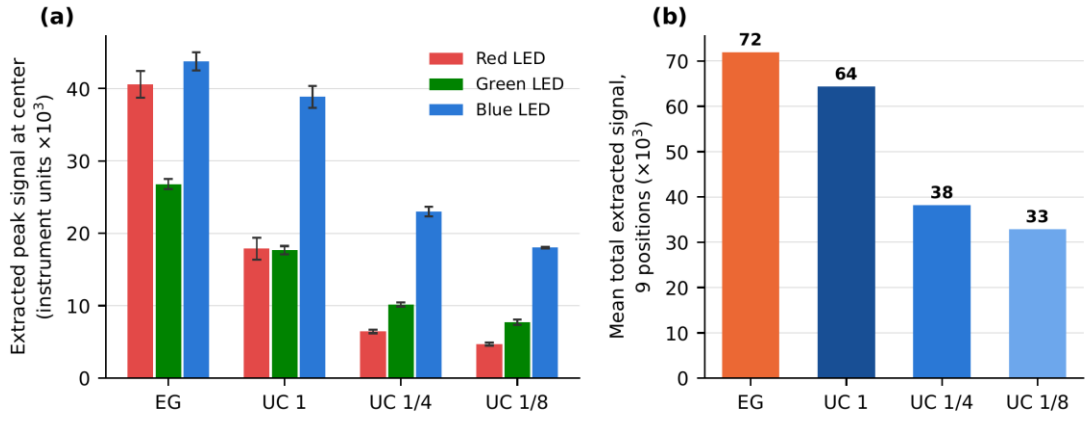


Fig. 8 Cross-filter extraction comparison under identical LED drive. (a) Per-channel extracted peak signal at the plate center (error bars: ±1 sd, n = 3); UC extraction is blue-dominant, EG is nearly neutral. (b) Total-extraction metric averaged over the nine grid positions.

4 Discussion

The two architectures present complementary trade-offs for electronically tunable in-camera tint synthesis. The EG filter has the lower insertion loss, the stronger passive veil and the flatter transmission spectrum, but its output under edge injection is not resolvably different (ratio ≈1.1 against a coupling uncertainty of up to 2×), so the substantive difference lies less in raw output than in how that output is delivered: a near-neutral, position-stable channel balance and a smooth, band-shaped brightness profile whose axis is set by the extraction pattern rather than by the injection geometry. A UC plate instead needs a strong, grade-dependent red boost that is exact at only one field position, because the long-wavelength absorption that produces its blue-shifted peaks also depletes the guided red light as it propagates. Against that, the UC family offers a calibration axis the EG filter does not: haze scales linearly with declared grade, so any edge-lit plate can be quoted in UC-equivalent units by measuring its haze and inverting the fit — though placing the EG filter at 1.64±0.27 extrapolates beyond the highest grade measured. The two profiles fail differently: the EG veil is strongest along the mid-height band and holds a constant hue across the frame, whereas the UC veil is both brighter and redder near one edge. The choice of the preferable behavior depends on the use case.

4.1 Limitations

Repetition counts are modest (n = 2–6). One filter of each type was measured: a single EG plate, and one plate of each UC grade. Architecture-level claims therefore rest on single samples, and the plate-to-plate systematics visible in Sec. 3.4 — UC 1/8 is less flat than UC 1/4 in every channel — indicate that sample variation is comparable to some of the smaller effects reported. The flux actually injected into each plate edge was not measured, so cross-filter extraction ratios assume equal strip-to-edge coupling; for the EG filter this assumption carries an uncertainty of up to ≈2×, because the LED strip was refixed between sessions and the single-color scans changed brightness accordingly. The LED drive current and junction temperature were also not controlled as tightly as they could have been; more precise current and temperature control would improve repeatability. The UC-equivalence figure rests on a three-point linear fit with one degree of freedom. It is extrapolated beyond the highest grade measured. A real UC filter of the suggested grade might behave differently. Imaging-side effects of the etched structures — diffraction

artifacts, modulation transfer function (MTF), ghosting, and stray-light artifacts — were not yet measured and require a camera-based test [2,13–15].

5 Conclusions

We compared a purpose-built etched-glass waveguide filter (CEZAMAT / Warsaw University of Technology) with three grades of the Tiffen Ultra Contrast family of filters as edge-lit, electronically tunable tint filters. The EG filter offers the lowest insertion loss (7.1 % over the 400–700 nm band), the strongest passive veil, a near-neutral and position-stable RGB extraction balance, and a band-shaped extraction profile showing that its one-dimensional coverage grading slightly overshoots a flat field on the axis it acts on while leaving the orthogonal axis uncompensated. The UC family is predictable passively — haze scales linearly with declared grade — but edge-lit, it is strongly blue-dominant and extracts red light far less uniformly than blue, so the veil hue varies across the frame. The two architectures therefore differ in the character of the veil rather than in its quantity: the etched waveguide delivers a neutral, position-stable veil at lower insertion loss, while UC 1/4 remains the flattest plate tested (min/max 0.76 versus 0.43 for EG). Future work will measure the injected flux for absolute efficiency figures and characterize imaging-side effects (diffraction artifacts, MTF, ghosting, and stray-light artifacts) with the filters mounted on a camera. The etched-glass extraction profile is also a design variable — the coverage grading is currently one-dimensional and can be re-specified on both axes and re-etched toward a flatter field — whereas the laminated filters offer only the manufacturer's discrete grade steps.

Disclosures

Jakub Duczmalewski is employed by ATM System, which commissioned the etched-glass filter examined here and commercially rents cinematographic filters and camera equipment. Mateusz Szczesny is employed by Quantitative Engineering Design (QED), the manufacturer of the ScanSpectrum spectrometer used for all measurements reported here. Joanna Starobrat, Maciej Sypek, Jarosław Suszek, and Filip Włodarczyk are with the Faculty of Physics, Warsaw University of Technology. The etched-glass filter was designed and fabricated at CEZAMAT, Warsaw University of Technology. The Tiffen Ultra Contrast filters were purchased on the open market; the authors have no relationship with The Tiffen Company, which had no role in the design, execution, or reporting of this study. To support independent verification, the underlying

spectrometer scans and the analysis code that generates every figure and quantitative value in this paper are available from the corresponding author on reasonable request (see Code, Data, and Materials Availability).

Funding

This research received no external funding.

Code, Data, and Materials Availability

The spectrometer scans underlying every figure and quantitative value in this paper, and the analysis code that produces them, are available from the corresponding author on reasonable request. The fabrication mask of the etched-glass filter and the December 2022 profilometry report are the property of Warsaw University of Technology, and may be shared at their discretion. The profilometric maps, height traces and patch dimensions reproduced in Fig. 3 are published with the permission of their author.

Acknowledgments

The authors thank the CEZAMAT team for supplying the fabrication mask and the profilometric survey of the etched plate. The profilometric survey reproduced in Fig. 3 was carried out at CEZAMAT by Filip Włodarczyk, who released it for publication here. Claude (Anthropic) was used for manuscript editing, for consistency checking of the reported values against the underlying measurement data, and for revision of the figure-generation scripts; all measurements, analyses, interpretations, and conclusions are the authors'.

References

1. International Organization for Standardization, "Optics and optical instruments — Veiling glare of image forming systems — Definitions and methods of measurement," ISO 9358:1994 (1994).
2. E. C. Fest, Stray Light Analysis and Control, SPIE Press, Bellingham, Washington (2013).
3. E.-V. Talvala, A. Adams, M. Horowitz, and M. Levoy, "Veiling glare in high dynamic range imaging," ACM Transactions on Graphics 26(3), 37 (2007), doi:10.1145/1276377.1276424.
4. J. J. McCann and A. Rizzi, "Veiling glare: the dynamic range limit of HDR images," in Human Vision and Electronic Imaging XII, Proc. SPIE 6492, 649213 (2007), doi:10.1117/12.703042.
5. RED Digital Cinema, "Understanding Low Contrast Filters," RED 101 technical article, https://www.reddigitalcinema.com/red-101/low-contrast-filters (accessed August 19, 2026).

6. The Tiffen Company, “4 × 5.65-inch Ultra Contrast Filter,” product page, https://tiffen.com/products/4-x-5-65-ultra-contrast-filter (accessed August 19, 2026).
7. The Tiffen Company, “Tiffen Filters Overview,” https://tiffen.com/pages/tiffen-filters-overview (accessed August 19, 2026).
8. M. McLamb, Y. Li, S. Park, M. Lata, and T. Hofmann, “Diffraction gratings for uniform light extraction from light guides,” in HONET-ICT 2019: IEEE 16th International Conference on Smart Cities, 220–222 (2019), doi:10.1109/HONET.2019.8908123.
9. H. J. Cornelissen, D. K. G. de Boer, and T. W. Tukker, “Diffraction gratings for lighting applications,” in Proceedings of SPIE, 8835:88350I (2013), doi:10.1117/12.2024026.
10. M. Quesada, W. Senaratne, S. Li, and A. Sullivan, “All-glass micro-groove light guide plate by mask and etch,” Optical Materials Express 11(2), 497–508 (2021), doi:10.1364/OME.414102.
11. A. Khan, “Dynamic lens filter and illuminated filter tray assembly,” U.S. Patent 12,216,384 B1 (2025).
12. QED, “ScanSpectrum,” product information page, https://about.qed.ai/scanspectrum (accessed August 19, 2026).
13. G. Kuwabara, “On the flare of lenses,” Journal of the Optical Society of America 43(1), 53–57 (1953), doi:10.1364/JOSA.43.000053.
14. S. Matsuda and T. Nitoh, “Flare as applied to photographic lenses,” Applied Optics 11(8), 1850–1856 (1972), doi:10.1364/AO.11.001850.
15. J. E. Greivenkamp, Field Guide to Geometrical Optics, SPIE Press, Bellingham, Washington (2004).

Jakub Duczmalewski leads the R&D and Service Department at ATM System, Warsaw, developing camera and lighting hardware for the film and broadcast industry. His current research focuses on electronically tunable, active in-camera optical filters, including the edge-lit etched-glass waveguide architecture developed with the Centre for Advanced Materials and Technologies (CEZAMAT), Warsaw University of Technology, where he also holds an MSc in Mechanical Engineering.

Mateusz Szczęsny is one of the key architects of the ScanSpectrum portable spectrophotometer. His work focuses on signal processing and machine learning, drawing on a background in medical imaging from his M.Sc. in Computer Science at the Faculty of Electronics and Information Technology, Warsaw University of Technology.

Joanna Starobrat is an Assistant Professor at Faculty of Physics, Warsaw University of Technology in Poland, who received her PhD degree in 2023 at the same university. She is a young researcher who has been interested in optics since she was a student, and has chosen holography and diffractive optics as her main area of research.

Jarosław Suszek Ph.D., Eng., is an Assistant Professor in the Optics and Photonics Division at the Faculty of Physics, Warsaw University of Technology. His research interests focus on diffractive and holographic optics, the design of diffractive optical elements, and the control of light propagation and spatial light distributions. His research combines numerical modelling, optical design, and experimental validation of microstructured optical elements aimed at generating advanced and innovative visual effects. His scientific work also includes applications of diffractive structures in imaging and photonic systems.

Filip Włodarczyk received the Eng. (2019) and M.Sc. (2021) degree from Faculty of Physics of Warsaw University of Technology in field of applied optical engineering. 2019-2021 gained optoelectronics experience in Łukasiewicz Research Group – Institute of Microelectronics and Photonics, focusing on nanostructured fibers and high-power fiber lasers. Currently is studying for PhD degree and conducting research at Warsaw University of Technology in field of diffractive optics and optical information processing.

Maciej Sypek is a Professor in the Faculty of Physics at Warsaw University of Technology (WUT), Poland. He received his Ph.D. and Habilitation from WUT, where he currently researches in the Optics and Photonics Division. His work focuses on diffractive optics, terahertz photonics, waveguiding, and nanophotonic structures. In addition to his academic research, he actively engages in technology transfer and industrial optical applications, including serving as CEO of Orteh Sp. z o.o.